Journal of Alloys and Compounds, 186 (1992) 347–359
JALCOM 290

The BaO–$TlO_{1.5}$ system

T. K. Jondo, R. Abraham, M. T. Cohen-Adad and J. L. Jorda
Université C. Bernard, Lab. Physico-Chimie Minerale II, 43 Blvd. 11 Nov. 1918, F-69622 Villeurbanne Cedex (France)

(Received February 24, 1992)

Abstract

The equilibrium phase diagram of the binary system BaO–$TlO_{1.5}$ under an oxygen pressure of 1 atm was studied by means of differential thermal analysis coupled with a thermobalance, X-ray diffractometry and plasma emission spectroscopy. Four intermediate phases have been identified: Tl_2BaO_4, $Tl_6Ba_4O_{13}$, $Tl_2Ba_2O_5$ and $TlBa_2O_{3.5}$. The congruent melting of $Tl_2Ba_2O_5$ offered a chance to prepare the superconducting cuprate $Tl_2Ba_2CuO_6$ avoiding the formation of $BaCuO_2$, a poisoning phase for reliable normal state studies at low temperatures.

1. Introduction

Amongst the high T_c superconductors the thallium series $Tl_mBa_2Ca_{n-1}Cu_nO_x$ ($m=1$, 2; $n=1$–5) are particularly interesting not only for the critical temperature record $T_c=130$ K [1] but also because they present a double series ($m=1$ and $m=2$) unique in these new materials and which may be interconnected by phase equilibria which have not yet been established. In fact, in the case of superconducting oxides the difficulties in obtaining a correct description of the phase diagrams are related to the number of components, the oxygen pressure and the lack of information on the simple binary systems. This is particularly true for the thallium cuprates, for which equilibrium in the BaO–$TlO_{1.5}$ system is still unknown. As may be seen in Table 1, at least six compounds have been identified from X-ray diffraction investigations [2–6] but there are doubts about the stability of some of them.

In this paper we determine the phase relations in the BaO–$TlO_{1.5}$ system. A simple extension to the ternary system BaO–$TlO_{1.5}$–CuO allows us to point out a method to prepare $Tl_2Ba_2CuO_6$ free of the usual impurity $BaCuO_2$.

2. Experimental details

Fifteen samples have been prepared starting from Tl_2O_3 (99.9%) and BaO_2 (99%) powders provided by Rhône-Poulenc. The firing and sintering

0925-8388/92/$5.00

TABLE 1

Reported compounds in the $TlO_{1.5}$–BaO system and structural characteristics

Compound Tl:Ba ratio	Cell type	Parameters (Å)	Reference
5:1	Orthorhombic	$a=17.676$ $b=24.167$ $c=10.110$	[6]
7:3	Orthorhombic	$a=17.724$ $b=6.890$ $c=10.235$	[6]
2:1	Orthorhombic	$a=10.446$ $b=12.200$ $c=3.498$	[2]
3:2	Orthorhombic	$a=5.748$ $b=7.221$ $c=9.361$	[5]
4:3	Hexagonal	$a=6.159$ $c=25.384$	[2]
1:1	Orthorhombic	$a=6.264$ $b=17.258$ $c=6.05$	[3]

treatments were carried out for 10–24 h in oxygen flowing at 750 °C, a temperature which is a compromise between dramatic thallium losses from Tl_2O_3 and necessary oxygen departure from BaO_2. The samples were cooled at a rate of 10 °C min^{-1} in order to ensure low temperature equilibrium. Some specimens were quenched in liquid nitrogen after subsequent heat treatments in sealed quartz tubes. The weight losses were carefully controlled and have been taken into account in the nominal compositions given subsequently.

The analytical determinations were as follows.

(1) X-ray diffraction (XRD) with a Siemens D520 apparatus using Cu Kα radiation. The intensities of the experimental diffraction lines were compared with the theoretical values of a LAZY-PULVERIX program adapted for personal computers [7].

(2) Differential thermal analysis coupled with a thermobalance (DTA–TG) operating in a controlled atmosphere. Most of the experiments were performed using alumina crucibles protected by a platinum sheet, with heating and cooling rates of 10 °C min^{-1}. In addition, isothermal measurements of the weight losses allowed a complementary analysis: a discontinuity in the weight loss rate (dm/dt) at a given temperature T as a function of time is connected with crossing phase fields and thus the presence of a given compound at this temperature in the equilibrium phase diagram may be ascertained. The process is better visualized by considering the derivative $(d^2m/dt^2)_T$ of the weight loss rate.

(3) Scanning electron microscopy with an energy-dispersive X-ray system attached. Semiquantitative analyses were obtained from the Mα and Lα lines of thallium and barium respectively.

(4) Plasma emission spectroscopy using Merck standard solutions.

3. Results and discussion

The results of the experiments are reported in Table 2 and may be summarized in the equilibrium phase diagram shown in Fig. 1. Four intermediate compounds have been unambiguously identified: Tl_2BaO_4, $Tl_6Ba_4O_{13}$, $Tl_2Ba_2O_5$ and $Tl_2Ba_4O_7$. We now examine the phase sequence in detail.

3.1. *The terminal fields*

The Tl_2O_3 powder used in this study melts at 762 °C, a value slightly lower than the 787 °C recently found by Wahlbeck *et al.* [8] with a high

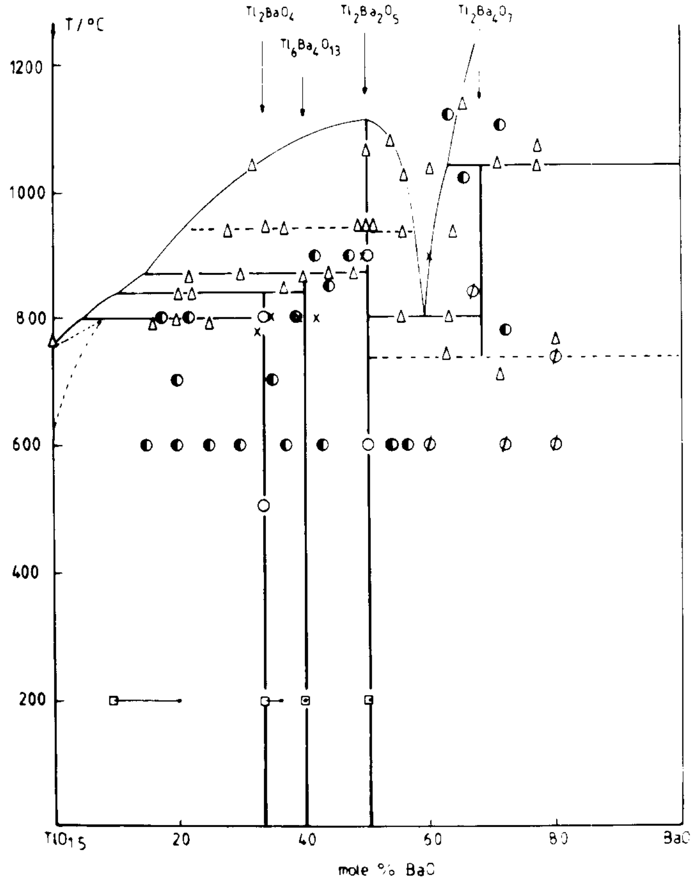

Fig. 1. The BaO–TlO$_{1.5}$ system in 1 atm pressure of oxygen: △, DTA peak; ×, isothermal thermogravimetry; ○, single phase, ◐, two phase, ∅ non-equilibrium three phase, □→ composition shift from plasma spectroscopy.

TABLE 2

Sample characterizations

Mol% BaO	DTA–TG		Analysis	
	T (°C)	BaO (%)		
14.3	795	16	XRD:	Tl_2O_3 ($a = 10.558$) + Tl_2BaO_4
	840	20	PS:	Tl:Ba = 4:1
	865	22	ITG	780 °C: BaO = 33%
	940	28		
	1040	32		
16.6			XRD:	Q(800 °C) Tl_2O_3 ($a = 10.531$) + Tl_2BaO_4
20	790	20	XRD:	Tl_2O_3 + Tl_2BaO_4
	845	22		Q(800 °C) $a(Tl_2O_3) = 10.532$
	865	30		Q(700 °C) $a(Tl_2O_3) = 10.51$
	940	34	ITG	900 °C: BaO = 49.5% and 60%
	1050	50		
	1080	54		
25	796	25	XRD:	Tl_2O_3 + Tl_2BaO_4
	855	30	ITG	800 °C: BaO = 35.2% and 42%
	940	37		
	1040	50		
	1080	54		
30			XRD:	Tl_2O_3 + Tl_2BaO_4
33.3	845	37	XRD	Q(800 °C, 900 °C): $Tl_6Ba_4O_{13}$ + $Tl_2Ba_2O_5$
	865	40	PS:	Tl:Ba = 1.7:1
	943	49	Sem-EDX:	Tl:Ba = 2:1
40	865	44	XRD	Q(850 °C, 900 °C): $Tl_6Ba_4O_{13}$ + $Tl_2Ba_2O_5$
	940	51		
	1020	55	PS:	Tl:Ba = 3:2
43	875	48	XRD:	$Tl_6Ba_4O_{13}$ + $Tl_2Ba_2O_5$
	940	50		
50	934	50	XRD:	Q(900 °C) $Tl_2Ba_2O_5$(LT)
	1050	61		Q(1000 °C, 1100 °C) $Tl_2Ba_2O_5$ (HT) + $Tl_2Ba_4O_7$
			PS:	Tl:Ba = 0.98:1
54			XRD:	$Tl_2Ba_2O_5$ + $BaO_{1.3}$
55.5	750	55	XRD:	$Tl_2Ba_2O_5$ + $BaO_{1.3}$
	930	55		
	1034	60.5		
	1127	66.5		
60	755	62.5	XRD:	$Tl_2Ba_2O_5$ + $BaO_{1.3}$ + X*
	800	62.5		Q(1020 °C)
	935	64		$Tl_2Ba_2O_5$ + $Tl_2Ba_4O_7$
	1042	71.5		Q(1100 °C) $Tl_2Ba_4O_7$ + BaO

(*continued*)

TABLE 2 (*continued*)

66.6	750	67	XRD:	Q(840 °C) $Tl_2Ba_4O_7$ $+ BaO_{1.3} + X^*$
71.4	750	71.5	XRD:	$Tl_2Ba_2O_5 + BaO_{1.3} + X^*$
	1035	77		Q(775 °C) $Tl_2Ba_4O_7 + BaO_{1.3}$
	1054	77		
80	765	80	XRD:	$Tl_2Ba_2O_5 + BaO_{1.3} + X^*$ Q(775 °C) $Tl_2Ba_4O_7 + X^*$ $+ Tl_2Ba_2O_5$

XRD, X-ray diffraction. When the temperature is not specified, the samples were slowly cooled after a homogeneity anneal and non-equilibrium may be observed, mainly for BaO-rich samples, (∅ symbols of Fig. 1). Q(... °C) means quenched in liquid nitrogen from ... °C. X* is an unidentified phase, probably in the ternary Tl–Ba–O system. The lattice parameters are given in angstroms.

PS, plasma spectroscopy; ITG, isothermal thermogravimetry; Sem-EDX, semiquantitative analysis by energy-dispersive X-rays; LT, low temperature; HT, high temperature.

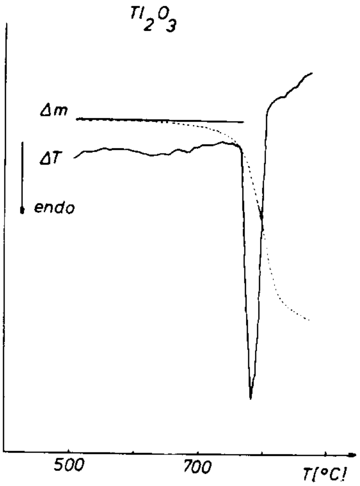

Fig. 2. DTA of Tl_2O_3 showing melting at 762 °C preceding severe decomposition. The heating rate is 10 °C min^{-1}.

purity (99.999%) oxide. Before melting, the weight loss of less than 2% cannot be due to complete decomposition of the sesquioxide in the monoxide Tl_2O and oxygen and therefore the DTA peak observed at 762 °C corresponds to the melting of Tl_2O_3. At higher temperature the material readily evaporates (Fig. 2), thus prescribing a firing temperature no greater than 760 °C. On cooling, solidification occurs without noticeable undercooling or weight increase. The crystal structure of Tl_2O_3 is cubic, space group *Ia*3, Mn_2O_3 type. All the diffraction lines could be indexed with a lattice parameter $a = 10.557(1)$ Å. Samples containing 12 and 20 mol% BaO and quenched from 795 °C in liquid nitrogen showed a contraction of the Tl_2O_3 cell,

$a = 10.531(9)$ Å, which suggests the possibility of barium substitution at the thallium sites. The limited solid solution is supported by the following peritectic reaction at 795 °C:

$$L + \langle Tl_2BaO_4\rangle \Longleftrightarrow (Tl_2O_3)$$

The DTA–TG in Fig. 3(a) reveal that the starting temperature for the decomposition of BaO_2 in oxygen flow is 600 °C. Figure 3(b) represents the weight loss rate dm/dT and indicates that at 750 °C the decomposition rate

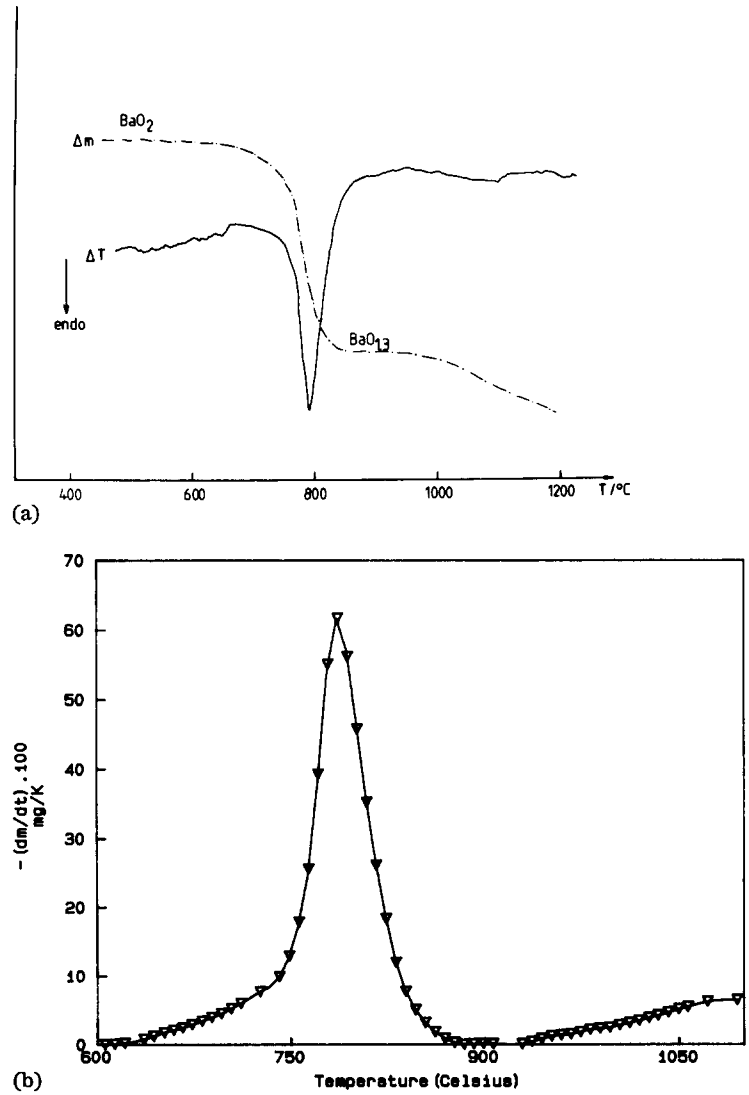

Fig. 3. (a) DTA of BaO_2. The peroxide decomposes at 600 °C but the weight change curve clearly indicates the formation of a suboxide corresponding to $BaO_{1.3}$. (b) Decomposition rate dm/dt as a function of temperature.

TABLE 3

XRD powder pattern of BaO_2 quenched from 900 °C. In fact, the oxide corresponds to $BaO_{1.3}$

d (Å)	I_{obs}
6.325	41
4.670	94
3.883	49
3.480	57
3.302	100
2.998	70
2.893	59
2.578	55
2.404	52
2.324	81
1.946	43
1.826	12
1.764	5
1.663	14
1.590	19

should allow complete formation of BaO in about 10 min. However, a stable state corresponding to $BaO_{1.3}$ is observed in the temperature range 800–1000 °C, BaO being obtained at higher temperature. The XRD pattern of $BaO_{1.3}$ quenched in liquid nitrogen from 900 °C is given in Table 3 and does not correspond to any known barium hydroxide or carbonate nor BaO hydrate. Considering the relationship between the BaO (NaCl-type) and BaO_2 (CaC_2-type) structures, an ordered distribution of molecular O_2 substituting for atomic oxygen in the BaO cell cannot be excluded, forming $BaO_{1.3}$ which could be of tetragonal symmetry. Inversely, on cooling as-quenched BaO from 1000 °C, oxygen capture starts at 400 °C. Consequently, in the BaO-rich field, results for the temperature range 400–1000 °C must be carefully analysed owing to the BaO–BaO_2 equilibrium and therefore the necessity to study the ternary Tl–Ba–O system.

3.2. *The compounds*

Four compounds have been observed in the system. We confirm the existence of Tl_2BaO_4 [2], $Tl_6Ba_4O_{13}$ [5] and $Tl_2Ba_2O_5$ [3–5] and we have identified a barium-rich compound $Tl_2Ba_4O_7$. $Tl_4Ba_3O_9$, mentioned by Lopato *et al.* [2], and the thallium-rich $Tl_{10}Ba_2O_{17}$ and $Tl_{14}Ba_6O_{27}$ phases recently described by Zhou *et al.* [6], could not be reproduced.

(1) Tl_2BaO_4 is formed at 840 °C by the peritectic reaction

$$L+\langle Tl_6Ba_4O_{13}\rangle \Longleftrightarrow \langle Tl_2BaO_4\rangle$$

The compound was first described by Lopato *et al.* [2] to be of the $CaFe_2O_4$-type structure with an orthorhombic cell $a=10.404$ Å, $b=12.12$ Å and $c=3.454$ Å. Recently Zhou *et al.* [6], on the basis of selected area electron diffraction (SAED) analysis, proposed a solid solution extending from

$Tl_5Ba_2O_{9.5}$ to Tl_2BaO_4. We have prepared a single-phase Tl_2BaO_4 by quenching a sample with nominal composition $(TlO_{1.5})_4(BaO)$ from 800 °C after 15 min annealing, while a stoichiometric Tl_2BaO_4 annealed for 12 h at 700 °C contained traces of $Tl_6Ba_4O_{13}$. A comparison of the XRD patterns of samples surrounding the single-phase Tl_2BaO_4 quenched from 800 °C is given in Table 4 and does not show significant modification of the *d* spacings, indicating, contradictory to Zhou *et al.*'s results, a reduced homogeneity range. All the diffraction lines may be indexed with an orthorhombic cell $a = 10.46(3)$ Å, $b = 11.93(3)$ Å and $c = 3.476(4)$ Å, but the experimental intensities do not match a $CaFe_2O_4$-type structure, space group *Pnma*.

(2) $Tl_6Ba_4O_{13}$, first mentioned by Zhou *et al.* [5], is confirmed here to be a stable compound in the $TlO_{1.5}$–BaO system. It is formed by the peritectic reaction

$$L + \langle Tl_2Ba_2O_5 \rangle \Longleftrightarrow \langle Tl_6Ba_4O_{13} \rangle \qquad (T = 865\ ^\circ C)$$

The isothermal experiment at 800 °C in Fig. 4 shows the change in weight loss rate, $-(d^2m/dt^2)$, as a function of time. It clearly reveals two constant regimes corresponding to the single-phase fields Tl_2BaO_4 and $Tl_6Ba_4O_{13}$. The latter may be easily distinguished from black Tl_2BaO_4 and $Tl_2Ba_2O_5$ owing to its yellowish-brown colour, but it is difficult to obtain a pure compound. All the XRD lines reported in Table 5 correspond to $Tl_6Ba_4O_{13}$ found as the main component in samples containing 37, 40 and 41.5 mol% BaO. The data were indexed as proposed by Zhou *et al.* [6] with an orthorhombic-

TABLE 4

XRD powder patterns of samples containing Tl_2BaO_4

Tl_4BaO_7 Q(700 °C)		Tl_2BaO_4 Q(800 °C)		$Tl_2Ba_{1.1}O_4$ A(500 °C)	
d (Å)	I_{obs}	*d* (Å)	I_{obs}	*d* (Å)	I_{obs}
		5.095	4	5.117	6
		3.207	6		
2.953	81	2.949	100	2.955	100
2.857	54	2.855	75	2.863	90
		2.479	4	2.484	8
		2.399	14	2.390	2
2.054	29	2.053	36	2.057	32
		1.999	3		
		1.751	4		
1.724	8	1.723	10	1.725	11
1.708	20	1.705	24	1.708	20
1.688	25	1.687	3	1.689	25
1.485	14	1.489	23	1.491	17
1.479	14	1.478	13	1.481	12

Q, quenched in liquid nitrogen; A, annealed and radiative cooling.

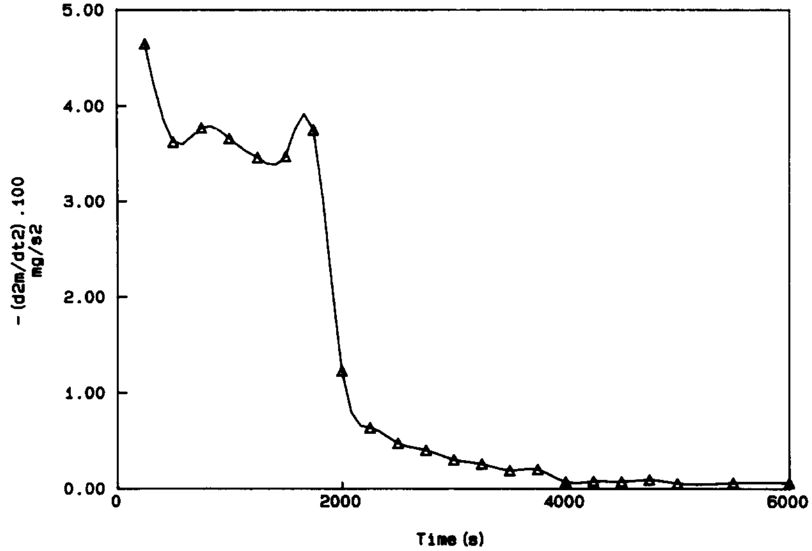

Fig. 4. Derivative of the weight loss rate (d^2m/dt^2) of initial $(TlO_{1.5})_{0.75}(BaO)_{0.25}$ at $T=800$ °C showing two breaks which correspond to Tl_2BaO_4 and $Tl_6Ba_4O_{13}$.

TABLE 5

XRD of nearly single-phase $Tl_6Ba_4O_{13}$ with proposed orthorhombic structure, $a=5.748$ Å, $b=7.164$ Å, $c=9.572$ Å

d (Å)	I_{obs}	*h k l*
7.164	59	0 1 0
4.786	15	0 0 2
3.731	9	1 0 2
3.310	15	0 2 1
3.059	24	1 2 0
2.874	100	2 0 0
2.788	11	1 0 3
2.560	35	1 2 2
2.396	12	0 0 4
2.328	9	2 1 2
1.911	20	3 0 0
1.718	11	1 4 0

type structure of slightly different cell size: $a=5.748$ Å, $b=7.164$ Å and $c=9.572$ Å.

(3) $Tl_2Ba_2O_5$: we found that the compound melts congruently at 1100 °C. First identified by Von Schenck and Muller-Buschbaum [3] with an orthorhombic $Ca_2Fe_2O_5$-type structure, space group *Pcmn*, the recent investigation of Zhou *et al.* [5] proposed a monoclinic distortion of the orthorhombic cell. Our data in Table 6 suggest a crystallographic modification from low to high ($T>950$ °C) temperature. The phase transition cannot be due to a composition shift. As a matter of fact, weight losses at 1000 °C

TABLE 6

XRD pattern of $Tl_2Ba_2O_5$ at low (LT) and high (HT) temperature

d_{LT} (Å)	I_{obs}	d_{HT}	I_{obs}
		5.24	22
		4.335	13
4.306	7	4.308	12
		4.222	12
		3.467	5
3.111	26	3.123	32
3.046	100	3.055	100
3.012	33	3.016	34
2.164	25	2.170	21
2.147	16	2.148	17
		2.103	4
1.785	19	1.790	15
1.768	10	1.771	10
1.746	30	1.750	23
1.639	5	1.643	4
		1.623	4
1.559	3	1.562	4
1.526	13	1.527	10
1.506	7	1.507	6

after a 5 min anneal in 1 atm of oxygen do not exceed 10%, thus shifting the composition towards $(TlO_{1.5})_{0.455}(BaO)_{0.545}$ in the two-phase field $Tl_2Ba_2O_5$ + liquid. Then a change in the XRD pattern of high temperature quenched samples supports a crystallographic modification in agreement with a DTA peak observed at 940 °C.

(4) $Tl_2Ba_4O_7$: in the BaO-rich field of the phase diagram we observed the formation of a new compound. From isothermal weight losses at 950 °C (Fig. 5) of an initial $Tl_2Ba_2O_5$ we propose for this compound the stoichiometry $Tl_2Ba_4O_7$. The XRD spectrum reported in Table 7 and compared with data in Table 3 shows that there is no possible confusion with the intermediate $BaO_{1.3}$ oxide with which $Tl_2Ba_4O_7$ is found to be in equilibrium at high temperature and especially at 1050 °C, the peritectic temperature. The compound seems to decompose peritectoidically at 750 °C, but it was already mentioned that the low temperature range of the BaO-rich side of the diagram is suspicious. From a crystallographic viewpoint, $Tl_2Ba_4O_7$ could be isotypic with tetragonal $Tl_2Sr_4O_7$ described by Von Schenck and Muller-Buschbaum [9] assuming the cell parameters $a = 5.33$ Å and $c = 23.04$ Å. However, some discrepancies between the experimental and computed intensities of the diffraction lines are observed. They may be explained by the presence of an impurity phase belonging to the ternary Tl–Ba–O system, reported as X* in Table 2.

As a conclusive remark concerning the phase sequence in the BaO–$TlO_{1.5}$ system, we note that each intermediate compound may be deduced from

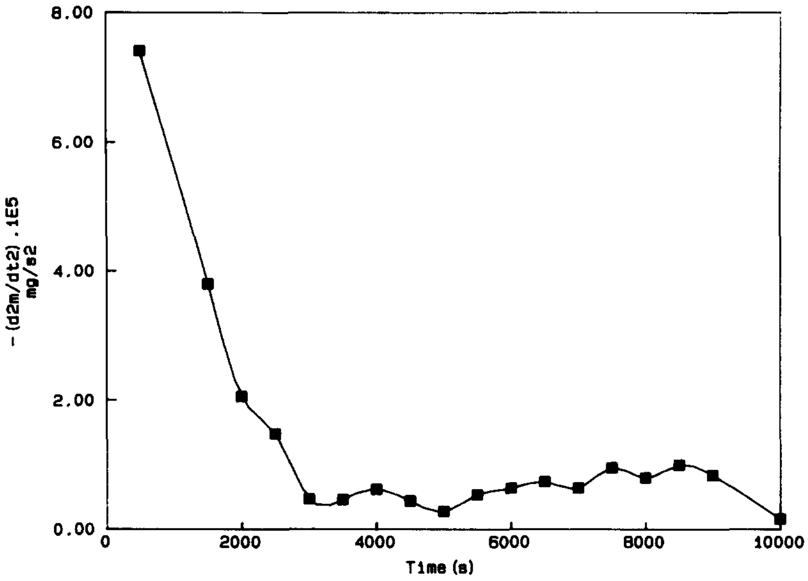

Fig. 5. Isothermal weight losses at 950 °C of $\mathrm{Tl_2Ba_2O_5}$. The discontinuity in the $\mathrm{d}^2m/\mathrm{d}t^2$ curve is attributed to crossing the $\mathrm{Tl_2Ba_4O_7}$ compound.

TABLE 7

Identification of $\mathrm{Tl_2Ba_4O_7}$ using the $\mathrm{Tl_2Sr_4O_7}$-type structure described in ref. 9 and the lattice parameters $a = 5.33$ Å, $c = 23.04$ Å

d_{obs} (Å)	I_{obs}	d_{th} (Å)	I_{th}	$h\ k\ l$
5.759	21	5.760	30	0 0 4
4.994	40			
3.772	24	3.769	1	1 1 0
3.527	49	3.582	50	1 1 2
3.159	40	3.154	100	1 1 4
2.973	17			
2.883	100	2.881	25	0 0 8
2.678	15	2.665	48	2 0 0
2.581	25	2.596	12	2 0 2
2.294	25	2.288	<1	1 1 8
1.962	2	1.966	30	1 1 10
1.889	81	1.884	21	2 2 0
1.743	1	1.744	1	2 1 9
1.714	5	1.710	10	1 1 12
1.666	2	1.667	13	3 1 2
1.611	18	1.618	35	3 1 4
1.583	22	1.583	18	2 2 8
1.397	1	1.400	14	2 0 11

Tl_2BaO_4 by the departure of 1 mole of Tl_2O_3 following the scheme

$$\begin{tikzcd}
4Tl_2BaO_4 \arrow[r] & Tl_6Ba_4O_{13}+Tl_2O_3 \arrow[d] \\
& 2Tl_2Ba_2O_5+Tl_2O_3 \arrow[d] \\
& Tl_2Ba_4O_7+Tl_2O_3
\end{tikzcd}$$

and therefore we see that the high temperature equilibrium will be strongly influenced by the Tl_2O_3 partial pressure.

3.3. *Extension to the ternary $TlO_{1.5}$–BaO–CuO system*

The congruently melting compound $Tl_2Ba_2O_5$ offers a chance to prepare the $Tl_2Ba_2CuO_6$ cuprate free of $BaCuO_2$ impurity. Indeed, the isoplethic line $Tl_2Ba_2O_5$–CuO has to be considered as a quasi-binary system and all samples on this line are expected to have a composition which must be solely a combination of $Tl_2Ba_2O_5$ and CuO. Thus $BaCuO_2$, the main impurity produced by sintering the elemental oxides, is not formed. In addition, owing to the relative stability of the mixed $Tl_2Ba_2O_5$ oxide comparatively to Tl_2O_3, thallium losses can be significantly reduced. The orthorhombic form of $Tl_{2-x}Ba_2CuO_6$ has been obtained with $x<0.05$. The compound is not superconducting and the normal state properties at low temperatures will be detailed elsewhere [10].

4. Conclusions

This study ascertains the existence of Tl_2BaO_4, $Tl_6Ba_4O_{13}$ and $Tl_2Ba_2O_5$ in the equilibrium phase diagram of the $TlO_{1.5}$–BaO system. A new compound corresponding to $Tl_2Ba_4O_7$ has been identified, but the structure, assumed to be isotypic to $Tl_2Sr_4O_7$, has yet to be confirmed. Except for the congruent melting $Tl_2Ba_2O_5$ which may be used as precursor for the preparation of superconducting thallium-based cuprates, all the compounds in the system are formed by peritectic reactions. The behaviour of BaO_2 in flowing oxygen, in particular the formation of an intermediate $BaO_{1.3}$ oxide, has to be taken into account on the BaO-rich side of the diagram.

References

1 T. Kaneko, H. Yamauchi and S. Tanaka, *Physica C, 178* (1991) 377.
2 L. M. Lopato, Z. A. Yaremenko and S. G. Tresvyatskii, *Ukr. Khim. Zh., 32* (1966) 437.
3 R. V. Von Schenck and H. K. Muller-Buschbaum, *Z. anorg. allg. Chem., 400* (1974) 197.
4 M. Itoh, R. Liang and T. Nakamura, *J. Solid State Chem., 82* (1989) 172.
5 W. Zhou, R. S. Liu and P. P. Edwards, *J. Solid State Chem., 87* (1990) 472.

6 W. Zhou, R. S. Liu and P. P. Edwards, *J. Solid State Chem.*, *91* (1991) 32.
7 K. Yvon, *LAZY-PULVERIX PC*, University of Geneva, 1988.
8 P. G. Wahlbeck, R. R. Richards and D. L. Myers, *J. Chem. Phys.*, *95* (1991) 9122.
9 R. V. Von Schenck and H. K. Muller-Buschbaum, *Z. anorg. allg. Chem.*, *396* (1973) 113.
10 J. L. Jorda, M. Couach, T. K. Jondo, R. Abraham, M. T. Cohen-Adad, C. Opagiste, A. Khoder and F. Sibieude, *Physica C.*